The Krüppel-Like Factor Gene Target Dusp14 Regulates Axon Growth and Regeneration

Joana Galvao,[1,2] Keiichiro Iwao,[*,3] Akintomide Apara,[3] Yan Wang,[2,3] Masoumeh Ashouri,[2] Tejas Nimish Shah,[2] Murray Blackmore,[†,3] Noelia J. Kunzevitzky,[1–4] Darcie L. Moore,[‡,3] and Jeffrey L. Goldberg[1–3]

[1]Byers Eye Institute, Stanford University, Palo Alto, California, United States
[2]Shiley Eye Center, University of California San Diego, La Jolla, California, United States
[3]Bascom Palmer Eye Institute, University of Miami Miller School of Medicine, Miami, Florida, United States
[4]Center for Computational Science, University of Miami, Miami, Florida, United States

Correspondence: Jeffrey L. Goldberg, Byers Eye Institute, Stanford University, 1561 Page Mill Road, Palo Alto, CA 94304, USA.

JG and KI contributed equally to the work presented here and should therefore be regarded as equivalent authors.

Current affiliation: *Kumamoto University, Kumamoto, Japan.
†Marquette University, Department of Biomedical Sciences, Milwaukee, Wisconsin, United States.
‡University of Wisconsin, Department of Neurosciences, Madison, Wisconsin, United States.

Submitted: November 8, 2017
Accepted: March 28, 2018

Citation: Galvao J, Iwao K, Apara A, et al. The Krüppel-like factor gene target Dusp14 regulates axon growth and regeneration. *Invest Ophthalmol Vis Sci*. 2018;59:2736–2747. https://doi.org/10.1167/iovs.17-23319

Purpose. Adult central nervous system (CNS) neurons are unable to regenerate their axons after injury. Krüppel-like transcription factor (KLF) family members regulate intrinsic axon growth ability in vitro and in vivo, but mechanisms downstream of these transcription factors are not known.

Methods. Purified retinal ganglion cells (RGCs) were transduced to express exogenous KLF9, KLF16, KLF7, or KLF11; microarray analysis was used to identify downstream genes, which were screened for effects on axon growth. Dual-specificity phosphatase 14 (Dusp14) was further studied using genetic (siRNA, shRNA) and pharmacologic (PTP inhibitor IV) manipulation to assess effects on neurite length in vitro and survival and regeneration in vivo after optic nerve crush in rats and mice.

Results. By screening genes regulated by KLFs in RGCs, we identified *Dusp14* as a critical gene target limiting axon growth and regeneration downstream of KLF9's ability to suppress axon growth in RGCs. The KLF9-Dusp14 pathway inhibited activation of mitogen-activated protein kinases normally critical to neurotrophic signaling of RGC survival and axon elongation. Decreasing Dusp14 expression or disrupting its function in RGCs increased axon growth in vitro and promoted survival and optic nerve regeneration after optic nerve injury in vivo.

Conclusions. These results link intrinsic and extrinsic regulators of axon growth and suggest modulation of the KLF9-Dusp14 pathway as a potential approach to improve regeneration in the adult CNS after injury.

Keywords: axon regeneration, Krüppel-like transcription factor, KLF, dual-specificity phosphatase 14, Dusp14, mitogen-activated protein kinases, MAPK, retinal ganglion cells, RGCs

Neurons in the adult mammalian central nervous system (CNS) fail to regenerate their axons after injury or in disease, while immature neurons regenerate robustly.[1,2] This phenomenon has been well-described in retinal ganglion cells (RGCs), the projection neurons of the eye that carry visual information to the brain via the optic nerve.[3] Regenerative failure of mature CNS neurons is thought to be due partly to a developmental loss in intrinsic growth capacity. We and others have shown that axon growth and regeneration is strongly modulated by transcription factors, such as Krüppel-like transcription factors (KLFs; KLF4, KLF7, and KLF9),[4–6] SRY-box containing gene (*SOXs*; *SOX11* and *SOX4*),[7–9] and activating transcription factors (ATFs; ATF3 and ATF2).[9–11] For example, knocking down KLF9, or interfering with its phosphorylation or interaction with JNK3, can promote long distance optic nerve axon regeneration.[6] Spinal cord axon regeneration can be induced by expression of KLF7, or more strongly by expression of a viral transcriptional activation domain fused to KLF7. Knocking out KLF4 developmentally or in adult RGCs promotes axon regeneration after optic nerve injury,[4,12] in part by eliminating its binding and inhibiting signal transducer and activator of transcription 3 (STAT3), which otherwise promotes axon growth via the Janus Kinase (JAK)-STAT3 signaling pathway.[12] However, gene targets downstream to these transcription factors have not been elucidated in neurons, and, thus, mechanisms downstream to KLFs in regulating intrinsic axon growth ability are not well understood.

In addition to intrinsic regulators of axonal growth, extrinsic factors, such as neurotrophins, ephrins, myelin-associated inhibitors, and chondroitin sulfate proteoglycan (CSPGs), influence axon growth capacity.[13] A major cause of regenerative failure after injury is thought to result from an interruption of neurotrophic supply. Neurotrophic factors are among the strongest regulators of axon growth developmentally[14,15] and promote growth and survival after injury.[16–22] Application of exogenous neurotrophins, such as ciliary neurotrophic factor (CNTF)[14,19,21,23] brain-derived neurotrophic factor (BDNF),[14,22] nerve growth factor (NGF),[24,25] neurotrophin-3,[13] and neurotrophin-4/5,[22,26] promote survival and axonal growth, often via

mitogen activated kinase (MAPK) signaling. Similarly, directly manipulating MAPK family members (ERKs, JNKs, p38, and DLK) in RGCs[27–32] can improve survival, axon growth, and regeneration.

How intrinsic and extrinsic factors interact to jointly regulate developmental growth and regeneration after injury is not well understood. We investigated genes downstream of KLFs family members, to determine the axon growth-relevant gene targets and pathways regulated by these transcription factors. We discovered that KLF9 drives expression of dual specific phosphatase-14 (DUSP14), and that DUSP14 dephosphorylates MAPK family members and its downregulation or inhibition blocks the axon growth inhibitory effects of KLF9 in vitro and promotes axon regeneration after optic nerve crush in vivo. This study uncovered a novel intrinsic transcription factor–mediated regulation of extrinsic neurotrophic signaling pathways and created a molecular link between these in the regulation of survival, axon growth, and regeneration.

Methods

Constructs for Transfection and Virus Transduction

For microarray analysis of RGCs, the open reading frames of *KLF9*, *-16*, -7, and *-11* were cloned from plasmids obtained from Open Biosystems (Huntsville, AL, USA). All 4 *KLFs* and FLAG-tagged *mCherry*[33] were cloned into pLenti-MP2 expression vector. For the screen in RGCs, plasmid constructs in pCMV-SPORT6 (Open Biosystems) were co-transfected with pmax-GFP (Lonza, Walkserville, MD, USA) and compared to co-transfection of control FLAG-tagged *mCherry*[33] with pmax-GFP. *Dusp14* and *KLF9* were obtained from Open Biosystems and cDNAs were subcloned into the *Spe*I/*Xba*I site in pLenti-MP2 expression vector with FLAG-mCherry or GFP tag. The phosphatase-dead mutant of *Dusp14* was obtained by substituting cysteine for serine at position 111 (C111S) using the QuikChange II XL Site-Directed Mutagenesis Kit (Agilent Technologies, Santa Clara, CA, USA). FLAG-tagged mCherry-pLenti-MP2 was used as control vector. To suppress Dusp14 expression in vivo, an inducible RNA polymerase II promoter[34] was subcloned upstream of four target shRNAs against the rat *Dusp14* gene (Gene Bank accession, BC158555) using target sequences as follows: 5′-TCGGATGATTTCCGAGGGAGA-3′, 5′-CTGACAAGATCCACAGTGTAA-3′, 5′-CTGGAGGCAGCTGATAGACTA-3′ and 5′-TGGCATCATTCCAGACGTTTA-3′. These four shRNA sequences in a SIBR cassette[34] were concatenated into a single vector and inserted into pAAV2 vector backbone, which also expresses eGFP as a transduction marker. Anti-luciferase shRNAs in the same pAAV2 system (kind gift from Vance P. Lemmon, University of Miami, Miami, FL, USA) were used as controls. All constructs were verified by sequencing.

RNA Preparation, Microarray Hybridization and Data Analysis

RGCs from early postnatal (P4) rats were purified and KLF9, -16, -7, and -11 genes and control, FLAG-tagged *mCherry* gene were transduced using lentivirus described as above. Total RNA was extracted (RNeasy; Qiagen, Valencia, CA, USA) independently and shipped to the National Institutes of Health (NIH, Bethesda, MD, USA) Neuroscience Microarray Consortium (University of California Los Angeles, Los Angeles, CA, USA), where it was amplified and processed for hybridization onto rat genome arrays (GeneChip Rat Genome 230 2.0 Array; Affymetrix, Santa Clara, CA, USA). At least five microarrays were used for each condition. RNA collected from independent samples obtained on different days served as the starting material for each microarray. Raw data files were normalized using the quantile method with GeneSpring GX 11 software (Agilent Technologies). Normalized data were filtered by percentile of intensity. Only the probes between the 20th and 99th percentiles in at least 50% of the samples per condition were considered for further analysis. Statistical comparison between conditions was performed using unpaired Student's *t*-test with Benjamini-Hochberg correction for multiple testing. Final data analysis was conducted using Excel software (Microsoft Corporation, Redmond, WA, USA). All raw data files are available at the NIH GEO Database - Series ID # GSE92507.

For screening, we selected KLF family gene targets that met the following criteria: (1) upregulated gene expression at least 3-fold by neurite growth-suppressive factor KLF9; (2) upregulated at least 1.5-fold by neurite growth-suppressive KLF16; (3) downregulated at least 1.5-fold by neurite growth-promoting factor, KLF7; and (4) no change in gene expression by KLF11. Full-length clones were from an Open Biosystems (Thermo Fisher Scientific, Huntsville, AL, USA) library maintained by Vance Lemmon, University of Miami. Transfected RGCs were identified by co-transfection with pmax-GFP (Lonza), and FLAG-tagged mCherry was used as a control. Co-transfection efficiency of pmax-GFP and FLAG-mCherry construct was 84.7 ± 1.2% in the beta-tubulin positive RGCs.

Purification, Culture, and Transfection of Primary RGCs

RGCs (P0 through P8) were purified by immunopanning as described previously.[14,15,35,36] RGCs were plated onto PDL- and laminin-coated tissue culture plates in growth media[14] including a homemade supplement similar to B27,[37] forskolin (5 mM), BDNF (50 ng/mL) and CNTF (10 ng/mL). In some experiments, protein tyrosine phosphatase (PTP) inhibitor IV (EMD Millipore, Billerica, MA, USA) was used as a pharmacologic Dusp14 inhibitor.[38] PTP inhibitor IV dissolved in dimethyl sulfoxide (DMSO) or DMSO control solutions were added at various concentrations 2 hours after electroporation and plating. RGCs were cultured in 10% CO_2 for 48 hours to analyze neurite growth.

For electroporation, after purification, 500 K RGCs were resuspended in electroporation solution containing 2 μg total DNA (GFP reporter and gene of interest in a 1:9 ratio), placed in a small cell number cuvette (Sigma-Aldrich Corp., St. Louis, MO, USA) and electroporated using Amaxa program SCN#1. Immediately following electroporation, growth media was added and the whole solution placed into a small Eppendorf tube. RGCs were centrifuged for 16 minutes at 300*g* (1800 rpm in an Eppendorf 5415D centrifuge) before resuspension and plating. For siRNA electroporation, 500 K postnatal rat RGCs were electroporated immediately after purification either with negative control or anti-Dusp14 siRNAs (Rn_Dusp14_predicted_1 and Rn_Dusp14_predicted_2; Qiagen), 500 nM per electroporation reaction in 27 μL electroporation solution and 2 μL (2 μg) transfection DNA (KLF9 or control). All siRNAs were validated for knockdown effect by immunohistochemistry using isolated RGCs (data not shown). RGCs were cultured in 10% CO_2 for 48 hours to quantify cell neurite growth.

For viral transduction of RGCs, 2500 P8 RGCs/well were plated on PDL/laminin-coated 48-well plates. At 16 hours after plating, AAV2 virus was diluted 1:1500 in media and added to cultured cells. Full media changes were performed 5.5 hours following virus exposure. For neurite growth assays, RGCs were fixed in 4% paraformaldehyde 5 days after initial addition of AAV2 viruses. The titer of AAV2 viruses ranged from 2.0 to 3.0×10^{13} genome copies/mL.

Investigative Ophthalmology & Visual Science

Immunohistochemistry

For cultured neurons, cultures were fixed using prewarmed 37°C 4% paraformaldehyde (PFA). For sections, frozen 15 μm sections were fixed with 4% PFA. Following rinses in PBS, samples were blocked and permeabilized in 20% normal goat serum (NGS) or 20% normal donkey serum with 0.02% Triton X-100 in antibody buffer (150 mM NaCl, 50 mM Tris base, 1% BSA, 100 mM L-lysine, 0.04% Na azide, pH 7.4) for 1 hour to reduce nonspecific binding. Samples were incubated overnight at 4°C in antibody buffer containing primary antibodies, washed with PBS, incubated in antibody buffer containing secondary antibodies and 4′,6-diamidino-2-phenylendole (DAPI) for 1 hour at room temperature, and washed with PBS. Cultures were left in PBS for imaging; sections were mounted using ProLong Gold Antifade Reagent (Molecular Probes, Inc., Eugene, OR, USA). Cultures were imaged for axon growth as below; sections were examined using confocal laser microscopy (TCS SP5, Leica or Zeiss 710; Carl Zeiss Meditec, Jena, Germany) and fluorescence microscopy (Observer.Z1; Carl Zeiss Meditec).

Primary antibodies used for these experiments included anti-β tubulin antibody from E7 hybridoma (1:500; Developmental Studies Hybridoma Bank, Iowa City, IA, USA), anti-β-III tubulin (1:500, 5568; Cell Signaling Technology, Danvers, MA, USA), anti-FLAG (1:250; Sigma-Aldrich Corp., F7425 and F1804), anti-GFP (1:200, A11122; Invitrogen, Carlsbad, CA, USA and GFP-1020; Aves Labs, Tigard, OR, USA), anti-phospho-ERK1/2 (1:200, 4370S; Cell Signaling Technology), anti-Brn3a (1:300, MAB1585; Millipore), anti-RBPMS (1:300, 1830-RBPMS; PhosphoSolutions, Aurora, CO, USA) and anti-Dusp14 (1:150, ab110938; Abcam, Cambridge, UK). Secondary antibodies were Alexa Fluor 488-, 594-, or 647-conjugated, highly cross-adsorbed antibodies (1:500; Invitrogen) and FITC-conjugated anti-chicken Igγ antibody (1:500, F-1005; Aves Labs).

Number of pERK-positive cells per 100 μm in the RGC layer and the fluorescence intensity of pERK per area in the RGC and inner plexiform layer were compared between control retinas and retinas with Dusp14 shRNA.

Quantification of Neurite Length and Neurite Number

For high content screening (HCS) of neuronal morphology, including average and maximum neurite lengths, neurite number and branching, automated microscopy (ArrayScan VTI, Thermo Fisher Scientific) and image analysis software (Cellomics Neuronal Profiling BioApplication; Thermo Fisher Scientific) were used to image and trace neurons using an ×5 or ×10 objective following immunostaining. RGCs were traced using β-tubulin immunoreactivity to visualize neurites. Neurons with dim signal in neurites were excluded from analysis, due to frequent tracing errors of faint processes; the threshold for exclusion was established using a population of negative control (Mock-transfected) immunostained RGCs. We previously validated this approach's consistency and reliability compared to hand-tracing.[4] Images and tracing were spot-checked to verify that the algorithms were correctly identifying neurites and quantifying growth.

Quantitative Reverse Transcription Polymerase Chain Reaction (qRT-PCR)

RGCs were purified by immunopanning and transduced with virus as above. At 48 hours after virus exposure for KLF9, cells were harvested and total RNA purified with RNeasy kit (Qiagen), subjected to reverse transcription (RT, iScript; Bio-Rad Laboratories, Hercules, CA, USA), and the resulting cDNA used as the template for a qPCR reaction (SsoAdvanced SYBR green; Bio-Rad Laboratories) performed on an iCycler (Bio-Rad Laboratories) with Dusp14 and 18S primers. Three repeat wells (technical replicates) were used for each condition. "No RT" control samples also were tested. The experiment was repeated four times with different pools of RNA (biological replicates). Primers used were as follows: Dusp14 forward: 5′ TCGAGATCCC CAACTTCAAC 3′; Dusp14 reverse: 5′ TGTCAGCCACAGTGT CAAAG 3′; 18S forward 5′ GAACTGAGGCCATGATTAAGA 3′; and 18S reverse: 5′ CATTCTTGGCAAATGCTTTC 3′.

Protein Extraction and Western Blot Analysis

RGCs were purified by immunopanning and transduced with virus as above. At 48 hours after lentivirus exposure for Dusp14 wild-type, Dusp14 C111S, KLF9, and FLAG-mCherry as a control, RGC proteins were extracted with radioimmunoprecipitation assay (RIPA) buffer containing protease and phosphatase inhibitor cocktails (Thermo Fisher Scientific). For collecting protein from in vivo retina, rats were deeply anesthetized and euthanized by inhalation overdose of CO_2 24 hours after optic nerve injury, and retina proteins were extracted with RIPA buffer containing protease and phosphatase inhibitor cocktails. Proteins in the cell extracts were separated by SDS-PAGE and electrotransferred to polyvinylidene fluoride (PVDF) membranes (Millipore) at 30 V for 60 minutes using the XCell SureLock Mini-Cell (Invitrogen). Membranes were blocked with chemiluminescent blocker (Millipore) and the antibody reaction performed with the SNAP i.d. system (Millipore). Primary antibodies used for these experiments included anti-phospho-ERK1/2 antibody (1:333; Sigma-Aldrich Corp.), anti-ERK1/2, anti-phospho-SAPK/JNK, anti-SAPK/JNK, anti-phospho-P38 MAPK, anti-P38 MAPK antibody (all 1:333; Cell Signaling Technology), and anti-GAPDH antibody (1:2000; Cell Signaling Technology). Secondary antibodies were horseradish peroxidase (HRP)–conjugated anti-mouse IgG and anti-rabbit IgG antibody (1:500; Santa Cruz Biotechnology, Dallas, TX, USA). Immunopositive bands were visualized by chemiluminescence with enhanced chemiluminescence (ECL; Thermo Fisher Scientific) and imaged on an LAS-3000 (Fujifilm, Tokyo, Japan). Densitometry was performed with Multi Gauge version 3.1 software (Fujifilm).

Animal Surgeries

Detailed protocols are available upon request. Animal experiments were conducted in accordance with the guidelines of the Institutional Animal Care and Use Committee (IACUC) and the Institutional Biosafety Committee of the University of Miami, University of California, San Diego, and Stanford University, and complied with the ARVO Statement for the Use of Animals in Ophthalmic and Vision Research.

Sprague-Dawley rats of varying ages and sex were obtained from Harlan Laboratories (Indianapolis, IN, USA). All surgeries were performed under adequate anesthesia with an intraperitoneal injection of ketamine hydrochloride, 60 mg/kg, and xylazine hydrochloride, 8 mg/kg body weight. Postoperatively, animals were allowed to recover on a heating pad and were given subcutaneous injections of buprenorphine hydrochloride, 0.1 mg/kg, twice a day for 3 consecutive days to minimize discomfort.

To inhibit Dusp14 expression, adeno-associated virus (seroform 2: AAV2) expressing Dusp14 shRNA was injected intravitreally (4.0 μL virus solution [titer, 7.0×10^{12}]) to the left eye at postnatal day 21 (P21) or Dusp 14 knockout (KO) mice were used. AAV2 expressing anti-luciferase shRNA and an eGFP reporter was injected in control eyes. One week after injection, RGCs were retrogradely labeled with fluorogold

(FG; Fluorochrome) to study RGC survival, as described previously.[39] In brief, the animals were anesthetized and the skull was exposed by a midline incision. Bilateral 2-mm diameter craniostomies were placed 0.5 mm posterolateral to the sagittal and transverse sutures. A small piece of Gelfoam (Gelfoam, USP; Pfizer, New York, NY, USA) soaked in 4% FG then was placed on the surface of the superior colliculus. Two weeks after virus injection, the left optic nerve was exposed and crushed using fine forceps (Dumont #5) at 2.0 mm behind the optic nerve head for 10 seconds, avoiding injury to the ophthalmic artery. A surgeon, masked to the viral treatment, performed all optic nerve crush surgeries. Two days before the end of the study, we injected 4.0 μL of 10 μg/μL cholera toxin subunit B (Ct B -555, Molecular Probes, Inc.) as an anterograde tracer to visualize axons and nerve terminals originating from living RGCs. Rats with any significant postoperative complications (e.g., retinal ischemia, cataract) were excluded from further analysis. Two weeks after optic nerve injury, animals were deeply anesthetized and perfused with 4% PFA in PBS. Optic nerves and retinas were dissected and fixed in 4% PFA for 1 hour and subsequently washed in PBS. Optic nerves were cryopreserved by incubation in 20% sucrose at 4°C overnight before mounting in optimal cutting temperature compound (OCT). Longitudinal sections (10 μm) were made of the entire optic nerve and imaged with ×20 magnification objective as above. Pictures were taken, starting with the furthest regenerating axons and working backwards toward the crush site. Lines were drawn perpendicular to the long axis of the optic nerve 0.25, 0.5, 0.75, and 1.0 mm past the crush site (as applicable), and Ct B-positive axons between these lines were counted. Analysis of the total sum of regenerating fibers from all sections for each animal as well as the average number of axons at each measurement location/distance per number of sections were performed in a masked fashion. To study RGC survival, retinas were dissected at days 7, 10, and 14 and immunohistochemistry was performed against Brn3a (1:300, Millipore) and RNA binding protein with multiple splicing (RBPMS; 1:300, Phosphosolutions). Three images for each quadrant of the retina were acquired using 710 Zeiss Confocal microscope (Carl Zeiss Meditec) and quantified by a researcher blinded to the experimental condition. To evaluate phospho-ERK signaling, BDNF (5 μg/3 μL, human BDNF; PeproTech, Rocky Hill, NJ, USA) was injected intravitreally immediately after optic nerve crush. For sectioning, rats were deeply anesthetized and euthanized 3 days after optic nerve injury. Rats with any significant postoperative complications (e.g., retinal ischemia, cataract) were excluded from further analysis.

Statistical Analysis

Data were analyzed using the JMP version 8 statistical package program (SAS Institute, Cary, NC, USA) or Graphpad Prism 6 (Graphpad, San Diego, CA, USA). The Tukey-Kramer honest significant difference (HSD) test was performed for multiple comparison for gene screening. For statistical comparison of two samples, we used a 2-tailed Student's *t*-test or paired *t*-test. *P* values of less than 0.05 were regarded as statistically significant.

Results

Microarray Analysis of KLF Family Members Identifies Dusp14 as Developmentally Regulated Axon Growth Suppressor

KLF-family Cys/His_2-type zinc finger domains bind similar DNA consensus sequences and demonstrate redundant and compensatory activities in regulating target genes and cellular phenotypes.[40] Since KLFs (e.g., KLF4) require their DNA binding domain to suppress axon growth,[4] and since multiple different KLFs have opposite effects on axon growth,[4,5] we hypothesized that identifying gene targets coordinately regulated by KLFs in neurons could unveil new pathways or mechanisms of axon growth regulation. We virally transduced purified postnatal day 4 (P4) RGCs[15,35] to overexpress single KLF family members, either axon growth suppressors (KLF9 or KLF16), an axon growth promoter (KLF7), or a control KLF family member that has no effect on axon growth (KLF11), or a control FLAG-mCherry construct.[4,5] Transcriptomes examined by Affymetrix microarray across five to six biological replicates of each KLF demonstrated low intersample variability (Supplementary Fig. S1). Of the targets probed, 21% changed at least 1.5-fold in at least one condition compared to FLAG-mCherry. Remarkably, 99.6% of the 1556 targets regulated by axon growth suppressors KLF9 and KLF16 showed expression changes in the same direction, and 86% of the 1139 targets regulated by axon growth suppressor KLF9 and axon growth enhancer KLF7 changed in the opposite direction (Fig. 1A), suggesting that KLFs' similar (KLF9 and -16) or opposing (KLF9 and -7) effects on axon growth are largely preserved in their coordinated regulation of gene expression. KLF regulation of other KLFs did not, however, demonstrate this consistency (Supplementary Table S1), pointing to a complexity in their cross-regulation.

We hypothesized that genes that change similarly in response to KLF9 and KLF16 (axon growth suppressors), but in the opposite direction in response to KLF7 (axon growth promoter), and not in response to KLF11 (no effect on axonal growth), might be the best candidates to identify direct or indirect KLF gene targets key in regulating intrinsic axon growth ability (Fig. 1B). A total of 27 genes satisfied those criteria (Supplementary Table S2). We selected the subset with full-length clones available from the National Institutes of Health Mammalian Gene Collection and expressed them individually in primary rat RGCs using GFP for a co-transfection marker, FLAG-tagged *mCherry* as a control, and automated image acquisition and neurite tracing for rapid and unbiased quantification of neurite growth.[4,41] We found that Dusp14 strongly suppressed neurite growth, decreasing the average neurite length to 72% (Fig. 1C) and decreasing the maximum length of neurites to 66% (Fig. 1D) with no effect on neurite number (Fig. 1E). These effects were remarkably similar to those seen in KLF9-transfected RGCs (Figs. 1C–E). For this reason and since we had previously identified KLF9 as a major regulator of axonal growth[6] further exploration of other KLFs' effects on Dusp14 expression was deferred.

We next investigated Dusp14 expression through retinal development, from postnatal day 0 (P0) to adult. KLF9 expression is developmentally upregulated 250-fold in RGCs after birth.[4] By immunofluorescence, no expression of Dusp14 was detected in the retina at P0. By P8, Dusp14 was detectable in RGCs (identified by Brn3a staining) and increased through development into adulthood (Fig. 1F). At P21 and in adult retina, Dusp14 also was detected in cells located on the inner side of the inner nuclear layer, but no expression of Dusp14 protein was detected in photoreceptor cells, retinal pigment cells or vascular endothelial cells. qRT-PCR showed Dusp14 expression increased 4-fold after KLF9 transduction compared to control (Fig. 1G). Conversely, knocking down KLF9 in vivo after intravitreal AAV2-anti-KLF9-shRNA (using constructs previously validated at the mRNA and protein level)[6] decreased Dusp14 protein expression compared to control (red). Taken together, KLF9 is sufficient in vitro and necessary in vivo for Dusp14 expression, and the two genes increase along a similar time course through early postnatal development.

Investigative Ophthalmology & Visual Science

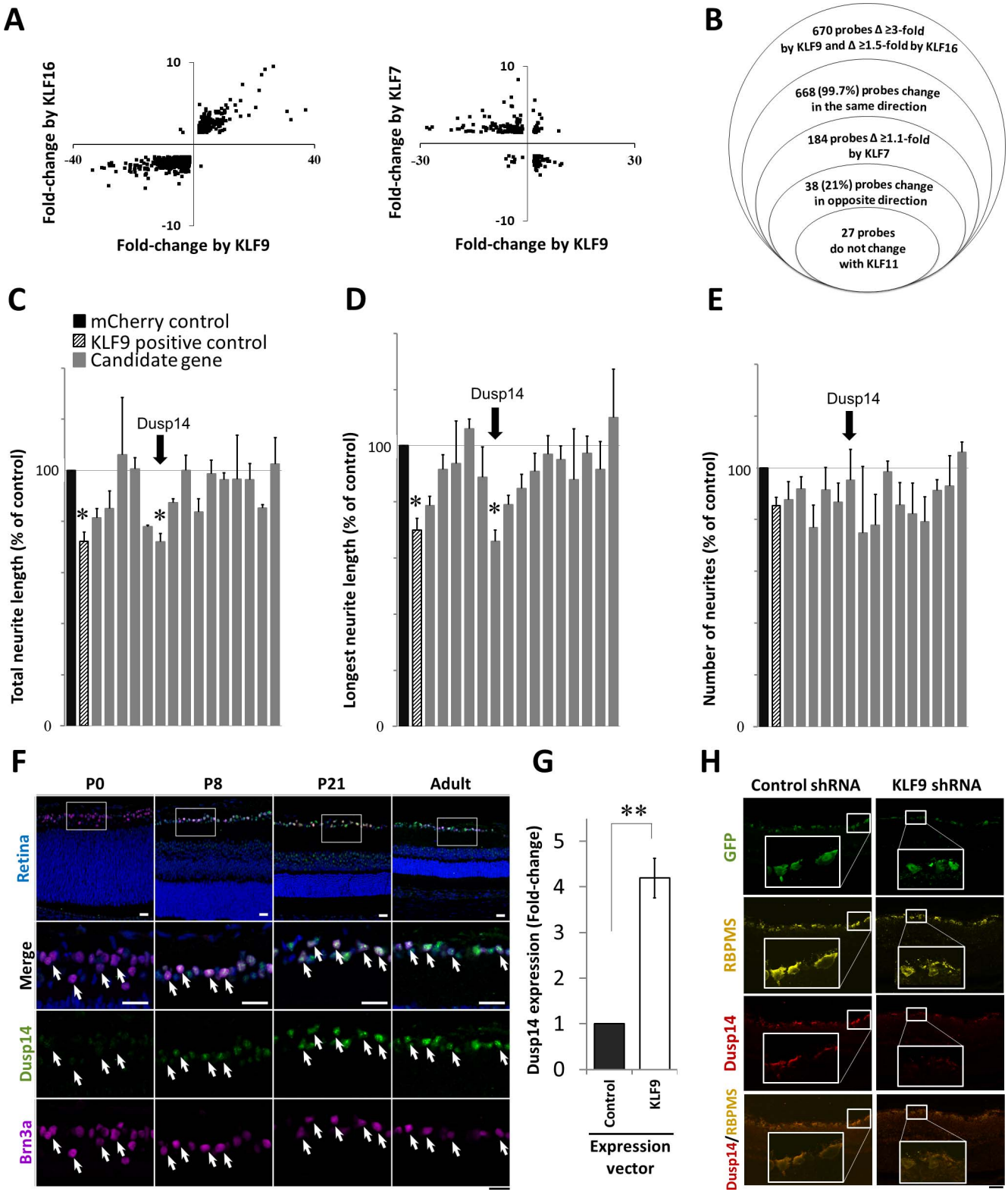

Figure 1. Microarray analysis and screening of candidate genes regulated by KLF family members identifies Dusp14 as developmentally regulated axon growth suppressor. (**A**) Scatterplots of KLF-regulated gene targets undergoing significant change in RGCs. (**B**) Modified Venn diagram characterizing gene expression analysis of RGCs expressing different KLF family members. (**C**–**E**) Gene expression effects on neurite growth screened in P0 RGCs. KLF9 (*pattern column*) and Dusp14 (*arrow*) decreased average and maximum neurite length with no effect on neurite number (*$P < 0.05$, Tukey-Kramer HSD test). (**F**) Dusp14 expression in the retina, at different postnatal ages. (**G**) qRT-PCR for Dusp14 in RGCs after KLF9 or control vector transduction (**$P < 0.01$, paired *t*-test; $n = 4$). (**H**) AAV2-anti-luciferase-shRNA (control shRNA) or AAV2-anti-KLF9-shRNA were intravitreally injected in adult rats and expressed in RGCs in vivo (GFP reporter, *green*). At 2 weeks, KLF9 shRNA led to a decrease in Dusp14 expression (*red*) in RGCs (labeled with RBPMS, *yellow*). *Scale bar*: 25 μm in (**F**) and 50 μm in (**H**). *Error bars*: standard error of the mean (SEM).

Investigative Ophthalmology & Visual Science

Dusp14 is Required for KLF9-Mediated Neurite Growth Suppression

KLF9 is the most highly developmentally regulated axon growth suppressor of the KLF family, increasing over 250-fold through RGC development.[4] Thus, we tested whether Dusp14 mediates KLF9's suppression of axon growth. In P0 RGCs, which do not express detectable levels of Dusp14 protein and express very low levels of KLF9 mRNA, two different Dusp14-specific siRNAs had, as expected, no effect on neurite growth. When we overexpressed KLF9, both Dusp14-specific siRNAs fully rescued P0 RGC neurite growth (Fig. 2A). In P8 RGCs, these siRNAs increased neurite growth in KLF9-overexpressing and control-transfected neurons (Fig. 2B), consistent with the endogenous expression of KLF9 and Dusp14 in these older neurons. Similarly, AAV2-anti-Dusp14-shRNA significantly increased neurite growth compared to control AAV2-anti-luciferase shRNA (Figs. 2C, 2D). We also examined pharmacologic inhibition of Dusp14 activity on neurite growth. PTP inhibitor IV, which effectively and specifically inhibits Dusp14-mediated dephosphorylation,[38] similarly promoted axon growth in a dose-dependent manner in control and KLF9-transfected P8 RGCs (Figs. 2E, 2F). Taken together, these results demonstrated that KLF9 requires expression of its target gene Dusp14 to suppress RGC axon growth ability.

Dusp14-Mediated Axon Growth Inhibition Depends on its Catalytic Activity

To determine the relevance of Dusp14's catalytic activity, we examined the effect of a point mutation at cysteine-111 to serine ($Dusp14^{C111S}$), which leads to loss of enzymatic dephosphorylation activity.[42] Dusp14's cysteine-111 residue catalyzes removal of phosphates initiated by a cysteine thiolate anion that attacks the tyrosine phosphate to form a cysteinyl-phosphate intermediate.[43] Compared to control transfected neurons, neurite growth was strongly suppressed in the KLF9- or Dusp14-transfected P4 RGCs (Figs. 3A–D). Co-transduction of KLF9 and Dusp14 showed stronger suppression of axon growth than KLF9 alone, but no significant inhibitory effect on neurite growth was observed in RGCs co-transduced with KLF9 and $Dusp14^{C111S}$ (Fig. 3D). To explore morphologic correlates of KLF9's and Dusp14's effects on inhibiting neurite growth, we quantified growth cone morphologies of RGCs overexpressing all four constructs. KLF9- and Dusp14-transfected RGCs demonstrated enlarged growth cones compared to control mCherry. The $Dusp14^{C111S}$ mutant had no effect on growth cone morphology or neurite growth (Figs. 3E, 3F). Growth cone size clearly is not related to inhibition versus elongation as this relationship may be context dependent,[44,45] but these data may help us understand the mechanism of effect to be explored in future studies. $Dusp14^{C111S}$ confers a dominant negative effect, preventing KLF9 expression from driving Dusp14-mediated suppression of axon growth, supporting the conclusion that Dusp14 is critical to KLF9-mediated axon growth suppression.

How does the KLF-Dusp14 pathway regulate axon growth? In nonneuronal cells, Dusp family members can inactivate mitogen-activated protein kinases (MAPKs), including ERK, JNK and P38 family members, through dephosphorylation at threonine and tyrosine residues (TXY motif) in the kinase domains.[42,46,47] MAPK proteins are critical for survival and axon growth of RGCs in vitro and in vivo,[15] and are activated by a variety of extracellular neurotrophic ligands that act on receptors at the cell body and the growth cone.[48] We investigated whether Dusp14 regulates MAPK phosphorylation in P0 RGCs, as little expression of Dusp14 was detected in vivo at that age (Fig. 1F). Expression of KLF9 or of Dusp14 led to dephosphorylation of members of all three MAPK families, pERK1/2, pJNK, and pP38 (Figs. 3G–J). In contrast, $Dusp14^{C111S}$ elicited no significant change in the phosphorylation of MAPKs (Figs. 3G–J). Therefore, KLF9 and Dusp14 lead to dephosphorylation of MAPKs, suggesting a hypothesis that this pathway limits axon growth by reducing intracellular signaling normally responsive to neurotrophic environmental cues.

Dusp14 Regulates RGC Survival and Optic Nerve Axon Regeneration In Vivo

First we asked whether Dusp14 expression is dysregulated after axon injury in vivo. Using a common model of optic nerve trauma, we found that surviving RGCs continued to express Dusp14 protein after optic nerve crush without significant change detectable by immunofluorescence at days 5 and 14 after injury (Fig. 4A). We evaluated molecular and cellular responses of RGCs to Dusp14 knockdown using AAV2-anti-Dusp14-shRNA vectors containing four concatenated anti-Dusp14 shRNAs, which transduced 93.3% of RGCs and, compared to control AAV2-anti-luciferase-shRNA, decreased expression of Dusp14 in RGCs at 2 weeks after intravitreal viral injection (Fig. 4B). Although the knockdown likely was not as complete as genomic KO would be,[49] we continued our studies with viral vectors to avoid developmental changes that could confound a full KO mouse, to maintain a greater measure of RGC-specificity, and to mimic the effect of treatment in the adult. We further found that Dusp14 shRNA significantly increased the number of BDNF-induced pERK-positive cells (Figs. 4C, 4D) and increased BDNF-dependent pERK signaling (Figs. 4E, 4F).

Finally, we evaluated the effect of knocking down Dusp14 expression on RGC survival and axon regeneration after optic nerve crush. Dusp14 knockdown promoted RGC survival at 7 days but not at 10 or 14 days after optic nerve crush in the adult rat (Figs. 5A, 5B). Interestingly, Dusp14 KO animal robustly promoted RGC survival 14 days after optic nerve injury (Figs. 5C, 5D). Dusp14 knockdown significantly increased the number and length of regenerating axons of RGCs in vivo (Figs. 5E, 5F). However, Dusp14 KO mice (Figs. 5G, 5H) and PTP inhibitor IV (data not shown) did not promote any significant increase in axon regeneration after axon injury. Thus, Dusp14 specifically suppresses axon regeneration in vivo after optic nerve injury, and targeting Dusp14 expression in RGCs with partial knockdown by shRNA promotes axon regeneration of RGCs.

Discussion

We identified Dusp14 as a critical player downstream of KLF9, mediating KLF9's axon growth suppressive effects on axon growth in vitro and contributing to inhibition of axon regeneration in vivo after optic nerve trauma. Furthermore, these data supported the hypothesis for the interaction between developmentally regulated, cell-intrinsic mediators of axon growth (e.g., KLFs), and extrinsic cues (e.g., neurotrophin-activated MAPKs). Enhancement of ERK phosphorylation stimulates neurite outgrowth and specific inhibitors of this pathway attenuate survival and neurite growth.[50] p38 MAPK signaling pathway also is implicated in neuritogenesis and regeneration,[51] and JNK signaling is involved in neurite initiation and elongation.[52,53] Interestingly, our own results showed increase in pJNK after optic nerve injury and that JNK3 binding domain is necessary for the KLF9-induced axon growth inhibition.[6] Thus, our data demonstrated that Dusp14 may decrease effects of all three contributing MAPK

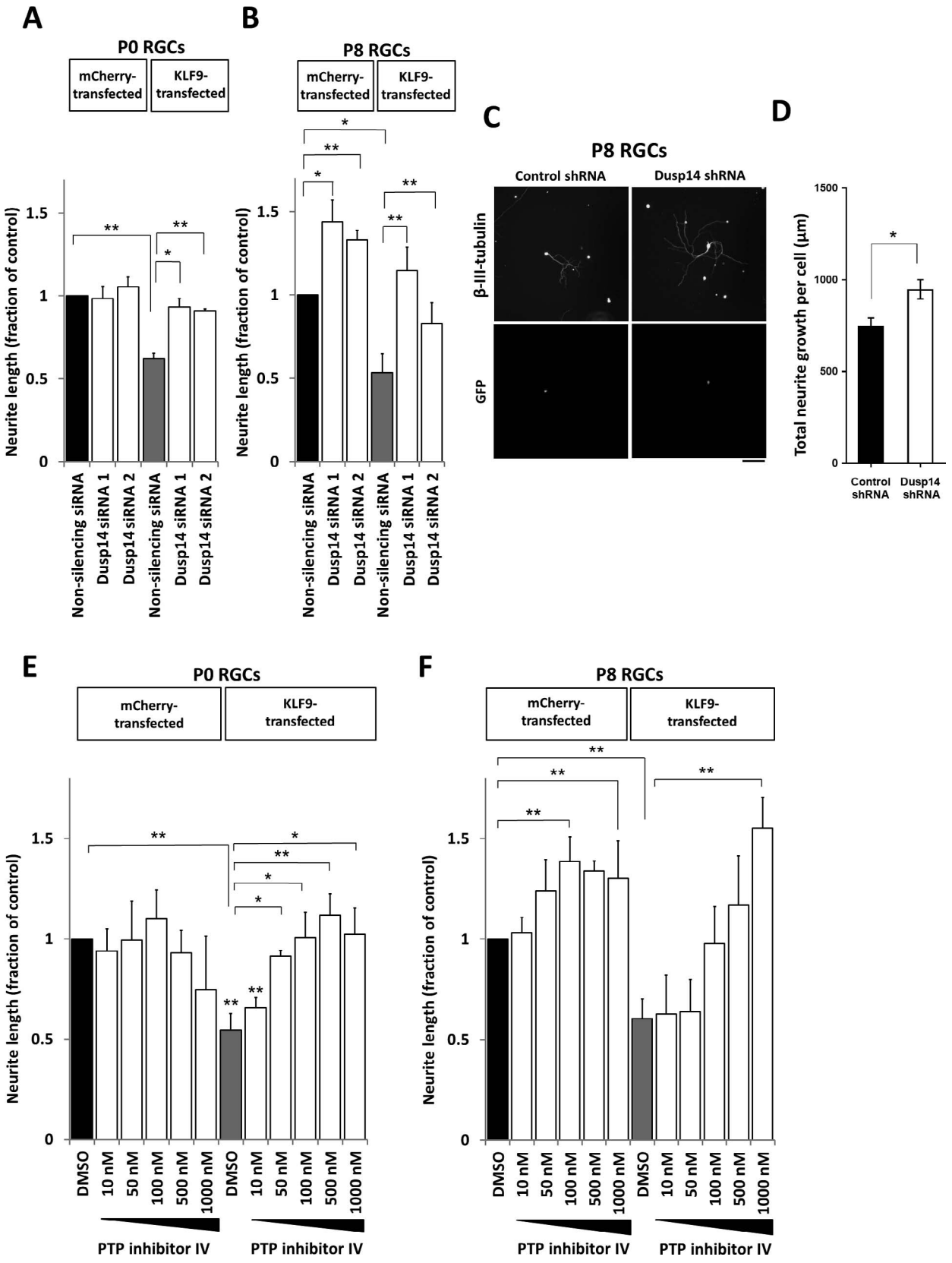

Figure 2. Rescue of KLF9-mediated neurite growth suppression by Dusp14 siRNA and PTP inhibitor IV. (**A**, **B**) At P0, control-transfected RGCs with no Dusp14 protein expression showed no effect when two different siRNAs against Dusp14 were transfected, in contrast to RGCs expressing higher levels of Dusp14 protein at P8, in which Dusp14 siRNAs significantly promoted neurite elongation. When overexpressing KLF9, siRNAs against Dusp14 rescued RGCs neurite growth at P0 (**A**) and P8 (**B**). (**C**, **D**) Similarly, AAV2 shRNA anti-luciferase (control shRNA) or AAV2 anti-Dusp14 (Dusp14 shRNA) were expressed in P8 RGCs. Dusp14 shRNA led to a significant increase in RGCs neurite growth. Images show staining against β-III-tubulin. Positively transduced RGCs were identified by a GFP reporter (**C**). Quantification showed significant increase in neurite growth after 5 days in culture (**D**). (**E**, **F**) PTP inhibitor IV (Dusp14 inhibitor) rescued KLF9-induced neurite suppression at P0 (**E**) and P8 (**F**), and promoted neurite growth in control-transfected RGCs at P8 (**F**), in dose-dependent fashion (*$P < 0.05$, **$P < 0.01$, paired *t*-test). *Scale bar*: 200 μm in (**C**). *Error bars*: SEM.

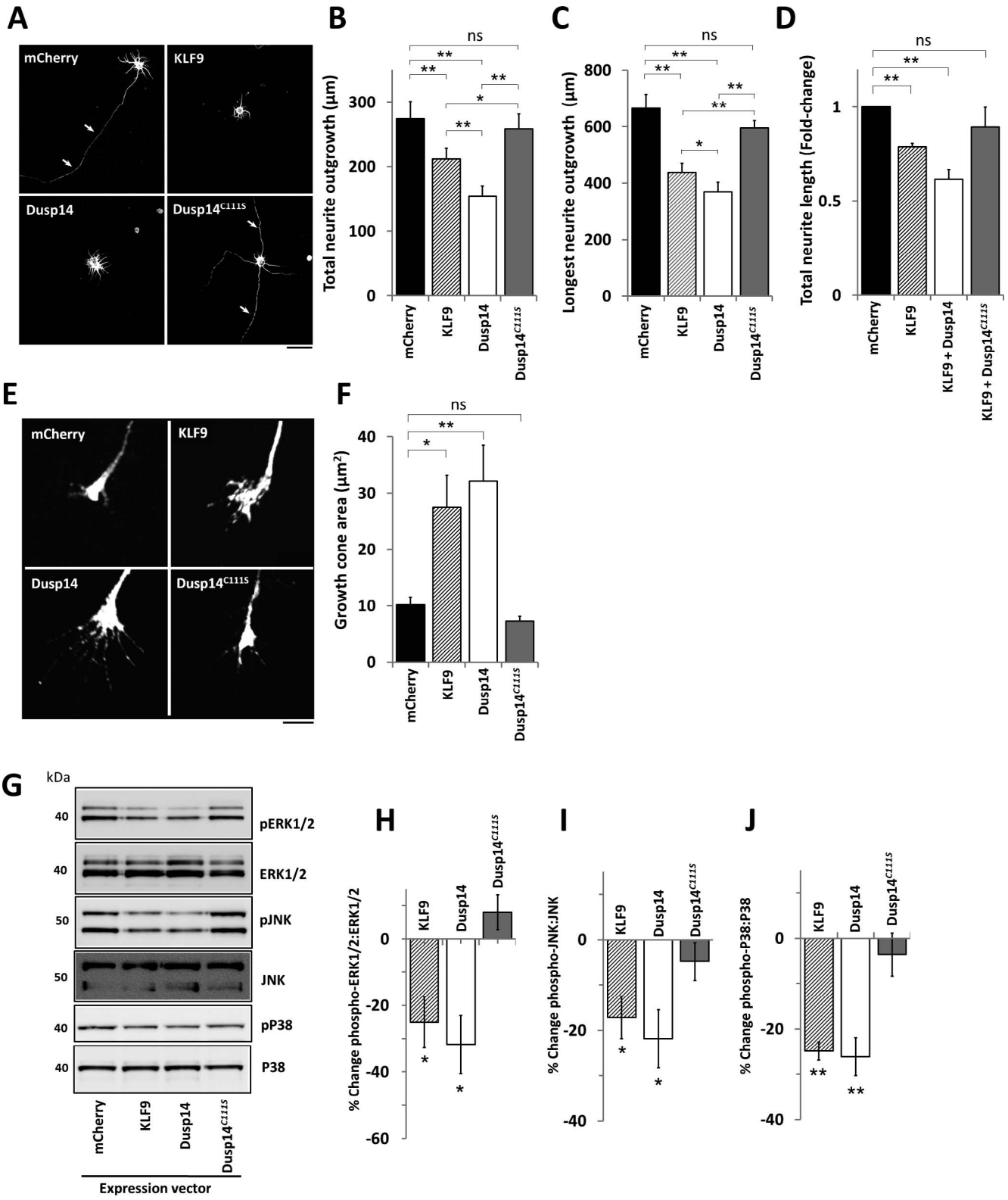

Figure 3. Dusp14 activity is required for Dusp14- and KLF9-induced RGC axon growth inhibition and MAPK dephosphorylation. (**A–D**) Neurite growth was inhibited by Dusp14 and KLF9 but not Dusp14^{C111S}. Neurite growth of RGCs co-transfected with KLF9 and Dusp14 or Dusp14^{C111S} (*$P < 0.05$, **$P < 0.01$, paired *t*-test). (**E**) Morphology of the growth cones of RGCs transfected with KLF9, Dusp14, and Dusp14^{C111S}. (**F**) RGCs transfected with KLF9 and Dusp14 led to enlarged growth cones, whereas Dusp14^{C111S} showed growth cones morphology similar with *mCherry* control. (**G**) Western blots for total ERK1/2, phospho- (p-) ERK1/2, total JNK, p-JNK, total P38 and p-P38 were analyzed in RGCs after gene transduction. (**H–J**) Densitometry of p-MAPK/total MAPK ratios: in Dusp14-transduced RGCs, the phosphorylation ratio of ERK1/2 (**H**), JNK (**I**), and P38 (**J**) were decreased 31.8%, 21.9%, and 26.1%, respectively. KLF9 induced a similar reduction of phosphorylation, but Dusp14^{C111S} showed no effect. (*$P < 0.05$, **$P < 0.01$ vs. control, paired *t*-test, $n = 4$; WT, wildtype). *Scale bar*: 5 μm in (**A**), 50 μm in (**E**). *Error bars*: SEM.

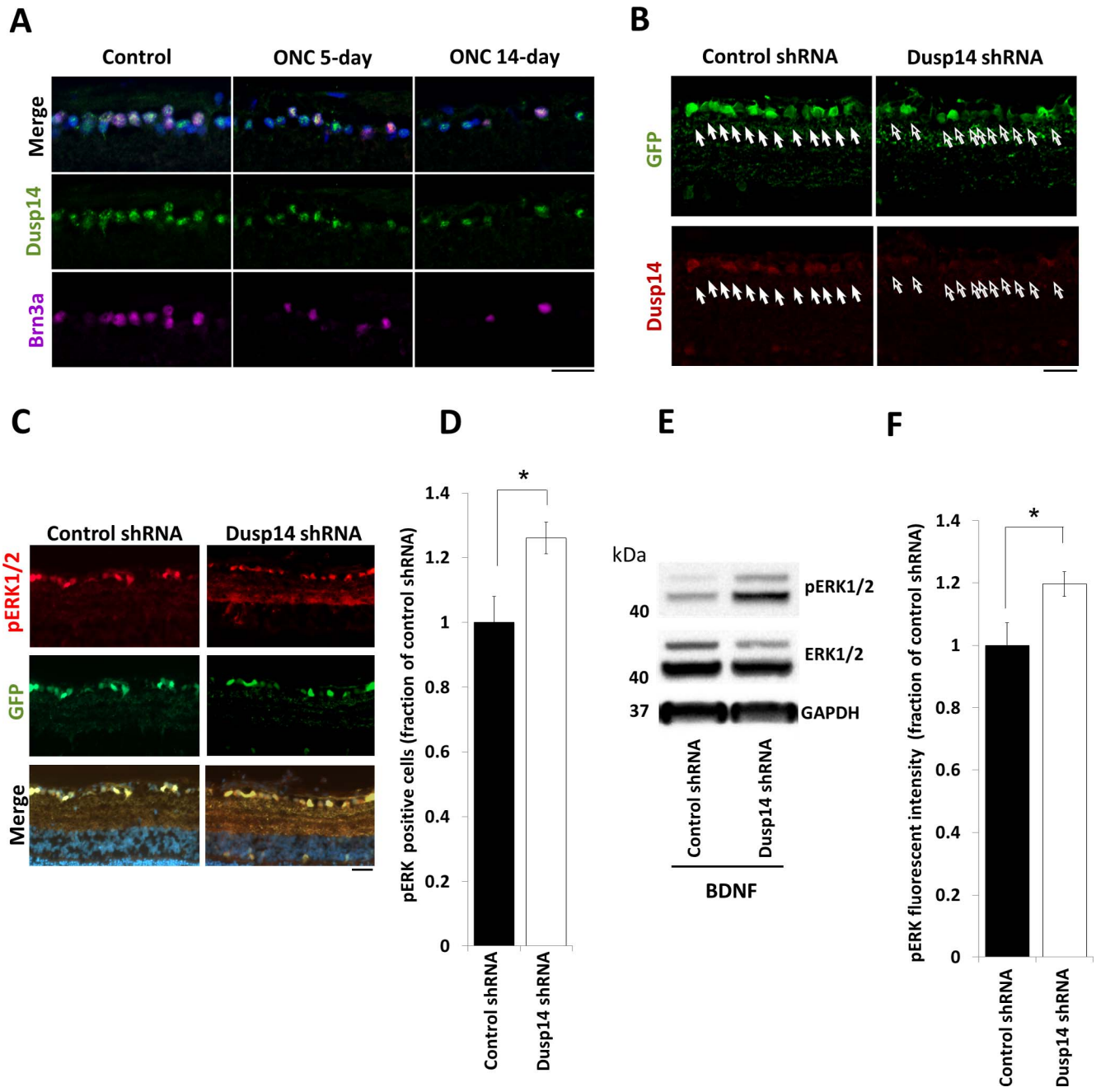

Figure 4. Dusp14 regulates axon regeneration through dephosphorylation of the MAPK family in vivo. (**A**) No change in Dusp14 expression was detectable at 5 and 14 days after optic nerve crush. (**B**) Dusp14 expression decreased after intravitreal injection of AAV2-Dusp14-shRNA in vivo (*arrows*). (**C**–**F**) Dusp14 knockdown significantly increased the number of pERK1/2-positive cells (**D**) and pERK1/2 fluorescent intensity (**E**) in retinas treated with BDNF. (*$P < 0.05$, Student's *t*-test; $n = 4$ [**D**, **E**]) *Scale bars*: 25 µm in (**A**) to (**C**), 500 µm in (**D**). *Error bars*, SEM.

signaling families (p38, ERK, and JNK), and at a minimum Dusp14 suppression significantly promotes BDNF-pERK signaling in RGCs in vivo. These data suggested that any residual or exogenously applied neurotrophic factors may have their pro-regenerative effects abrogated by Dusp14 expression in adult RGCs or other CNS neurons. Thus, the developmentally regulated expression of KLFs in adult CNS neurons may act to suppress neurotrophic factor signaling.

Other phosphatases have demonstrated activity in regulating neurite growth and regeneration, including phosphatase and tensin homolog (PTEN),[54] protein phosphatase A2 (PP2A),[55] and calcineurin.[56] Dual specific phosphatases (DUSPs) make up a subgroup of the class-I cysteine-based PTP superfamily that regulate divergent biological and pathological processes.[57] They are a family of 61 phosphatases with different tissue expression patterns and heterogeneous functions,[42] including specifically dephosphorylating MAPK family members, thereby inactivating them. Tight regulation of MAPK family members is critical to control growth after development.[46] While we found Dusp14 expression changed developmentally (Fig. 1F), and that Dusp14 expression is driven by KLF9 (Figs. 1G, 1H), it currently is unknown whether Dusp14 is directly or indirectly regulated by KLF9 or other KLFs. We did not observe any change in Dusp14 expression after optic

Investigative Ophthalmology & Visual Science

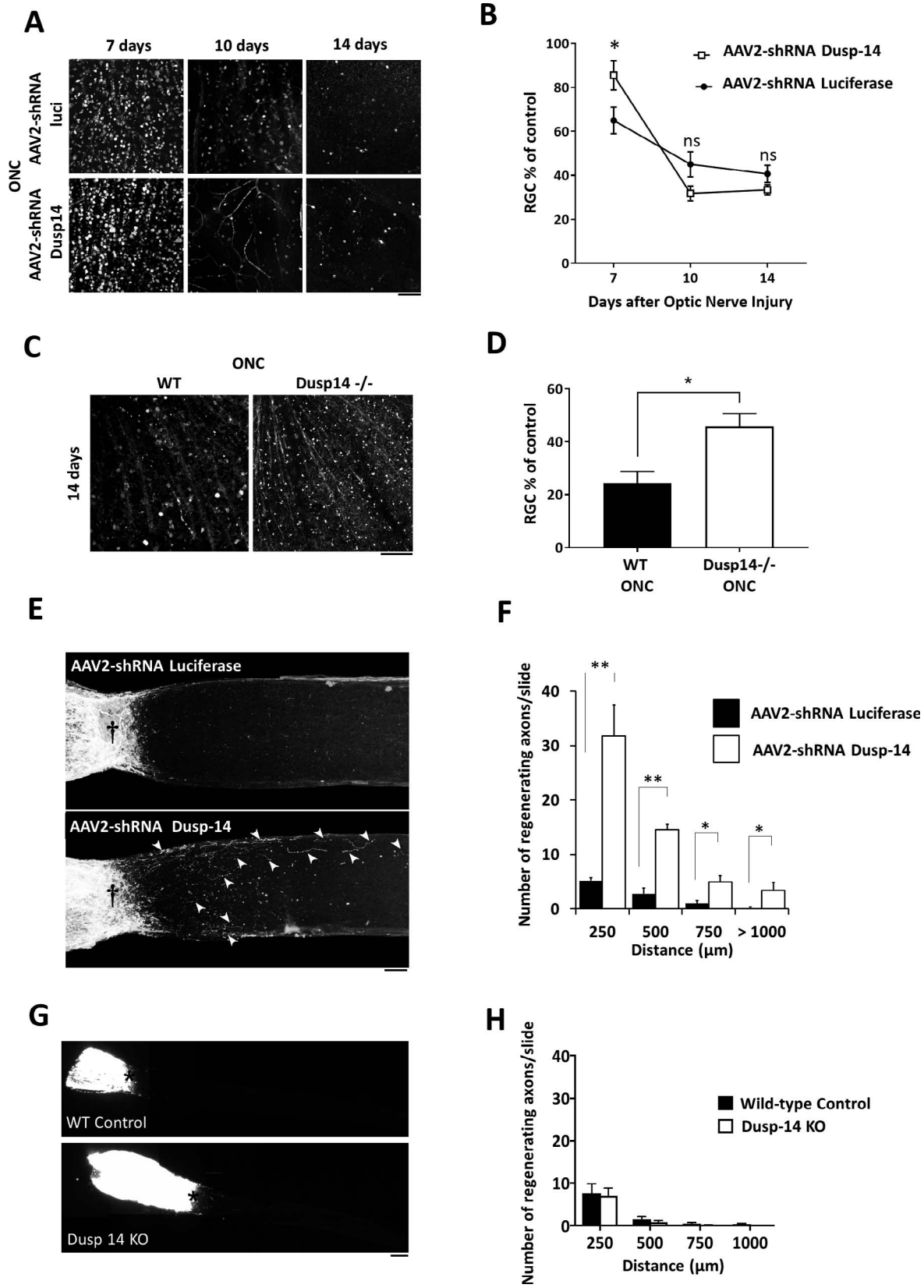

Figure 5. Dusp14 regulates optic nerve axon regeneration and RGC survival in vivo. (**A**) Images show RBPMS (RGC marker) staining of RGCs at days 7, 10, and 14 after optic nerve crush, for either AAV2-shRNA Luciferase or AAV2-shRNA Dusp14 injected rats. (**B**) Dusp14 shRNA promotes RGC survival at 7 days after optic nerve crush. (**C**) Images show RBPMS (RGC marker) staining of RGCs at day 14 after optic nerve crush, for either wild type control or Dusp14 KO mice. (**D**) Dusp14 KO promotes RGC survival at 14 days after optic nerve crush. (**E**) Partial projections of sectioned optic nerve from Dusp14 knockdown and control optic nerve. Regenerating axons (*arrowheads*) were observed in Dusp14 shRNA-treated optic nerves but not in controls. †Crush site. (**F**) Significantly more fibers regenerated after shRNA-mediated knockdown of Dusp14. (**G**) Example partial projections of sectioned optic nerve from Dusp14 KO mice and control optic nerve. (**F**) No difference was detected in the number of regenerating axons in Dusp14 KO compared to controls. *Crush site (*$P < 0.05$, **$P < 0.01$, 1-way ANOVA followed by Tukey's test; $n = 4$ [**A**, **B**]; $n = 5$ [**C**, **D**]). *Scale bars*: 100 µm in (**A**), 500 µm in (**C**). *Error bars*: SEM.

Investigative Ophthalmology & Visual Science

nerve injury, consistent with the premise that the developmental regulation of KLFs is the primary, cell-autonomous regulator of Dusp14 expression. Interestingly, our bioinformatics analysis did not reveal a consensus KLF response element upstream in the proximal promoter region of the DUSP14 locus. Other than Dusp14, no other Class-I PTPs, including other Dusp family members, were identified in our microarray data as potential downstream targets of KLF7, -9, -16, or -11. Hence, Dusp14 may be one of the few Class-I PTP genes regulated by KLFs that specifically regulate MAPK dependent growth and regeneration in RGCs or other CNS neurons.

Knocking down Dusp14 in vivo yielded less regeneration than manipulating KLF9 in vivo.[6] This could be explain by three reasons: first, KLF9 is a transcription factor that could be activating other unidentified inhibitory pathways in vivo that were not present or were not activated in vitro. Second, our in vitro results were obtained in purified RGCs from postnatal days 0 and 8 compared to manipulation of these factors in adult cells.[15] Third, to maintain RGCs in culture, the media must be highly supplemented with neurotrophic factors, such as BDNF and CNTF.[6,14] Additionally, neither developmentally knocking out Dusp14, nor using a pharmacologic inhibitor, had any effect on axon regeneration after injury. This may reflect a requirement for Dusp14 activity at low levels in RGCs (since there is residual expression after shRNA knockdown), and/or for Dusp14 activity in other retinal or optic nerve cells, or by a compensatory effect of other Dusp family member. Indeed Dusp6 and Dusp1 have high homology with Dusp14. As the effect of KLF9 knockdown is greater than that of Dusp14 KO, other targets of KLF9 should be explored in further studies on the differences in KLF biology within and across cells.

Taken together these data strongly supported the motivation to bridge biology and therapeutically target the interaction between cell-autonomous, developmentally regulated transcriptional regulators and the signaling pathways critical for regulating axon growth and regeneration. Further work linking the developmental switch in intrinsic axon growth ability to the extrinsic, glial-associated cues that limit survival and growth of neurons may lead to new therapeutic approaches to promote CNS repair after injury or in degenerative disease.

Acknowledgments

The authors thank Vance P. Lemmon for access to a cDNA library and for anti-Luciferase shRNA pAAV2 plasmid; Yan Shi, Raquibul Chowdhury, Pingping Jia, Eleut Hernandez, and Gabriel Gaidosh for technical assistance from; and Evan G. Cameron and Sahil Shah for scientific discussion.

Supported by the National Eye Institute (EY022129 to JLG; P30-EY026877, P30-EY022589, and P30-EY014801), Department of Defense (W81XWH-12-1-0254), an unrestricted grant from Research to Prevent Blindness, and the Uehara Memorial Foundation in Japan (to KI).

Disclosure: **J. Galvao**, None; **K. Iwao**, None; **A. Apara**, None; **Y. Wang**, None; **M. Ashouri**, None; **T.N. Shah**, None; **M. Blackmore**, None; **N.J. Kunzevitzky**, None; **D.L. Moore**, None; **J.L. Goldberg**, None

References

1. Bregman BS, Kunkegbagden E, Mcatee M, Neill AO. Extension of the critical period for developmental plasticity of the corticospinal pathway. *J Comp Neurol*. 1989;282:355–370.
2. Chen DF, Jhaveri S, Schneider GE. Intrinsic changes in developing retinal neurons result in regenerative failure of their axons. *Proc Natl Acad Sci U S A*. 1995;92:7287–7291.
3. Goldberg JL, Klassen MP, Hua Y, et al. Amacrine-signaled loss of intrinsic axon growth ability by retinal ganglion cells. *Science*. 2002;296:1860–1864.
4. Moore DL, Blackmore MG, Hu Y, et al. KLF family members regulate intrinsic axon regeneration ability. *Science*. 2009;326:298–301.
5. Blackmore MG, Wang Z, Lerch JK, et al. Krüppel-like Factor 7 engineered for transcriptional activation promotes axon regeneration in the adult corticospinal tract. *Proc Natl Acad Sci U S A*. 2012;109:7517–7522.
6. Apara A, Galvao J, Wang Y, et al. KLF9 and JNK3 interact to suppress axon regeneration in the adult CNS. *J Neurosci*. 2017;37:1–13.
7. Norsworthy MW, Bei F, Kawaguchi R, et al. Sox11 expression promotes regeneration of some retinal ganglion cell types but kills others report Sox11 expression promotes regeneration of some retinal ganglion cell types but kills others. *Neuron*. 2017;94:1112–1120.
8. Welsbie DS, Mitchell KL, Jaskula–Ranga V, et al. Enhanced functional genomic screening identifies novel mediators of dual leucine zipper kinase-dependent injury signaling in neurons. *Neuron*. 2017;94:1142–1154.
9. Moore DL, Goldberg JL. Multiple transcription factor families regulate axon growth and regeneration. *Dev Neurobiol*. 2011;71:1186–1211.
10. Tsujino H, Kondo E, Fukuoka T, et al. Activating transcription factor 3 (ATF3) induction by axotomy in sensory and motoneurons: A novel neuronal marker of nerve injury. *Mol Cell Neurosci*. 2000;15:170–182.
11. Herdegen T, Leah JD. Inducible and constitutive transcription factors in the mammalian nervous system: control of gene expression by Jun, Fos and Krox, and CREB/ATF proteins. *Brain Res Rev*. 1998;28:370–490.
12. Qin S, Zou Y, Zhang C-L. Cross-talk between KLF4 and STAT3 regulates axon regeneration. *Nat Commun*. 2013;4:2633.
13. Yiu G, He Z. Glial inhibition of CNS axon regeneration. *Nat Rev Neurosci*. 2006;7:617–627.
14. Meyer-Franke A, Kaplan MR, Pfrieger FW, Barres BA. Characterization of the signaling interactions that promote the survival and growth of developing retinal ganglion cells in culture. *Neuron*. 1995;15:805–819.
15. Goldberg JL, Espinosa JS, Xu Y, Davidson N, Kovacs GTA, Barres BA. Retinal ganglion cells do not extend axons by default. *Neuron*. 2002;33:689–702.
16. Isenmann S, Klöcker N, Gravel C, Bähr M. Short communication: protection of axotomized retinal ganglion cells by adenovirally delivered BDNF in vivo. *Eur J Neurosci*. 1998;10:2751–2756.
17. Harper MM, Grozdanic SD, Blits B, et al. Transplantation of BDNF-secreting mesenchymal stem cells provides neuroprotection in chronically hypertensive rat eyes. *Invest Ophthalmol Vis Sci*. 2011;52:4506–4515.
18. Mey J, Thanos S. Intravitreal injections of neurotrophic factors support the survival of axotomized retinal ganglion cells in adult rats in vivo. *Brain Res*. 1993;602:304–317.
19. Cui Q, Lu Q, So KF, Yip HK. CNTF, not other trophic factors, promotes axonal regeneration of axotomized retinal ganglion cells in adult hamsters. *Invest Ophthalmol Vis Sci*. 1999;40:760–766.
20. Leaver SG, Cui Q, Plant GW, et al. AAV-mediated expression of CNTF promotes long-term survival and regeneration of adult rat retinal ganglion cells. *Gene Ther*. 2006;13:1328–1341.
21. Müller A, Hauk TG, Leibinger M, Marienfeld R, Fischer D. Exogenous CNTF stimulates axon regeneration of retinal ganglion cells partially via endogenous CNTF. *Mol Cell Neurosci*. 2009;41:233–246.

22. Sawai H, Clarke DB, Kittlerova P, Bray GM, Aguayo AJ, Hospital G. Brain-derived neurotrophic factor and neurotrophin-4 / 5 stimulate growth of axonal branches from regenerating ganglion cells. *J Neurosci*. 1996;16:3887–3894.
23. Goldberg JL, Barres BA. The relationship between neuronal survival and regeneration. *Annu Rev Neurosci*. 2000;23:579–612.
24. Roberti G, Mantelli F, Macchi I, Massaro-Giordano M, Centofanti M. Nerve growth factor modulation of retinal ganglion cell physiology. *J Cell Physiol*. 2014;229:1130–1133.
25. Maffei L, Carmignoto G, Perry V, Candeo P, Ferrari G. Schwann cells promote the survival of rat retinal ganglion cells after optic nerve section. *Proc Natl Acad Sci U S A*. 1990;87:1855–1859.
26. Cohen A, Bray GM, Aguayo AJ. Neurotrophin-4 / 5 (NT-4 / 5) increases adult rat retinal ganglion cell survival and neurite outgrowth in vitro. *J Neurobiol*. 1994;25:953–959.
27. O'Brien GS, Sagasti A. Fragile axons forge the path to gene discovery: a MAP kinase pathway regulates axon regeneration. *Sci Signal*. 2009;2:pe30.
28. Andrusiak MG, Jin Y. Context specificity of stress-activated MAP Kinase signaling: the story as told by C. elegans. *J Biol Chem*. 2016;291:7796:7804.
29. Welsbie DS, Yang Z, Ge Y, et al. Functional genomic screening identifies dual leucine zipper kinase as a key mediator of retinal ganglion cell death. *Proc Natl Acad Sci U S A*. 2013;110:4045–4050.
30. Watkins TA, Wang B, Huntwork-Rodriguez S, et al. DLK initiates a transcriptional program that couples apoptotic and regenerative responses to axonal injury. *Proc Natl Acad Sci U S A*. 2013;110:4039–4044.
31. Hao Y, Frey E, Yoon C, et al. An evolutionarily conserved mechanism for cAMP elicited axonal regeneration involves direct activation of the dual leucine zipper kinase DLK. *Elife*. 2016;3:1–18.
32. Shin JE, Cho Y, Beirowski B, Milbrandt J, Cavalli V, DiAntonio A. Dual leucine zipper kinase is required for retrograde injury signaling and axonal regeneration. *Neuron*. 2012;74:1015–1022.
33. Shaner NC, Campbell RE, Steinbach PA, Giepmans BNG, Palmer AE, Tsien RY. Improved monomeric red, orange and yellow fluorescent proteins derived from Discosoma sp. red fluorescent protein. *Nat Biotechnol*. 2004;22:1567–1572.
34. Chung K, Hart CC, Al-bassam S, et al. Polycistronic RNA polymerase II expression vectors for RNA interference based on BIC / miR-155. *Nucleic Acids Res*. 2006;34:e53.
35. Barres B, Silverstein BE, Corey P, Chun L. Electrophysiological variation among retinal ganglion cells purified by panning. *Neuron*. 1988;1:791–803.
36. Hu Y, Cho S, Goldberg JL. Neurotrophic effect of a novel TrkB agonist on retinal ganglion cells. *Invest Ophthalmol Vis Sci*. 2010;51:1747–1754.
37. Chen Y, Stevens B, Chang J, Milbrandt J, Barres BA, Hell JW. NS21: re-defined and modified supplement B27 for neuronal cultures. *J Neurosci*. 2008;171:239–247.
38. Park JE, Park BC, Song M, et al. PTP inhibitor IV protects JNK kinase activity by inhibiting dual-specificity phosphatase 14 (DUSP14). *Biochem Biophys Res Commun*. 2009;387:795–799.
39. Chiu K, Lau W, Yeung S, Chang RC, So K. Retrograde labeling of retinal ganglion cells by application of fluoro-gold on the surface of superior colliculus. *J Vis Exp*. 2008;16:819.
40. Moore DL, Apara A, Goldberg JL. Kruppel-like transcription factors in the nervous system: Novel players in neurite outgrowth and axon regeneration. *Mol Cell Neurosci*. 2011;47:233–243.
41. Buchser WJ, Pardinas JR, Shi Y, Bixby JL, Lemmon VP. 96-Well electroporation method for transfection of mammalian central neurons. *Biotechniques*. 2006;41:619–624.
42. Patterson KI, Brummer T, O'Brien PM, Daly RJ. Dual-specificity phosphatases: critical regulators with diverse cellular targets. *Biochem J*. 2009;418:475–489.
43. Lountos GT, Tropea JE, Cherry S, Waugh DS. Overproduction, purification and structure determination of human dual-specificity phosphatase 14. *Acta Crystallogr Sect D Biol Crystallogr*. 2009;65:1013–1020.
44. Kurklinsky S, Chen J, MA M. Growth cone morphology and spreading are regulated by a dynamin-cortactin complex at point contacts in hippocampal neurons. *J Neurochem*. 2011;1117:48–60.
45. Goldberg JL. How does an axon grow? *Genes Dev*. 2003;17:941–958.
46. Jeffrey KL, Camps M, Rommel C, Mackay CR. Targeting dual-specificity phosphatases: manipulating MAP kinase signalling and immune responses. *Nat Rev Drug Discov*. 2007;6:391–403.
47. Huang C-Y, Tan T-H. DUSPs, to MAP kinases and beyond. *Cell Biosci*. 2012;2:24.
48. Steketee MB, Moysidis SN, Jin X-L, et al. Nanoparticle-mediated signaling endosome localization regulates growth cone motility and neurite growth. *Proc Natl Acad Sci U S A*. 2011;108:19042–19047.
49. Yang C-Y, Li J-P, Chiu L-L, et al. Dual-specificity phosphatase 14 (DUSP14/MKP6) negatively regulates TCR signaling by inhibiting TAB1 activation. *J Immunol*. 2014;1924:1547–1557.
50. Washio A, Kitamura C, Jimi E, Terashita M, Nishihara T. Mechanisms involved in suppression of NGF-induced neuronal differentiation of PC12 cells by hyaluronic acid. *Exp Cell Res*. 2009;315:3036–3043.
51. Verma P, Chierzi S, Codd A, et al. Axonal protein synthesis and degradation are necessary for efficient growth cone regeneration. *J Neurosci*. 2005;25:331–342.
52. Barnat M, Enslen H, Propst F, Davis RJ, Soares S, Nothias F. Distinct roles of c-Jun N-terminal kinase isoforms in neurite initiation and elongation during axonal regeneration. *J Neurosci*. 2010;30:7804–7816.
53. Tonges L, Planchamp V, Koch JC, Herdegen T, Bahr M, Lingor P. JNK isoforms differentially regulate neurite growth and regeneration in dopaminergic neurons in vitro. *J Mol Neurosci*. 2011;45:284–293.
54. Park KK, Liu K, Hu Y, et al. Promoting axon regeneration in the adult CNS by modulation of the PTEN/mTOR pathway. *Science*. 2008;322:963–966.
55. Monroe JD, Heathcote RD. Protein phosphatases regulate the growth of developing neurites. *Int J Dev Neurosci*. 2013;31:250–257.
56. Lautermilch NJ, Spitzer NC. Regulation of calcineurin by growth cone calcium waves controls neurite extension. *J Neurosci*. 2000;20:315–325.
57. Alonso A, Sasin J, Bottini N, et al. Protein tyrosine phosphatases in the human genome. *Cell*. 2004;117:699–711.

Investigative Ophthalmology & Visual Science